

Quantum engineering of atomic phase shifts in optical clocks

T. Zanon-Willette,^{1,2,*} S. Almonacil,³ E. de Clercq,⁴ A. D. Ludlow,⁵ and E. Arimondo⁶

¹*Sorbonne Universités, UPMC Univ. Paris 6, UMR 8112, LERMA, F-75005, Paris, France*

²*LERMA, Observatoire de Paris, PSL Research University, CNRS, UMR 8112, F-75014, Paris France*

³*Institut d'Optique Graduate School, 2 avenue Augustin Fresnel, 91127 Palaiseau Cedex, France*

⁴*LNE-SYRTE, Observatoire de Paris, CNRS, UPMC, 61 avenue de l'Observatoire, 75014 Paris, France*

⁵*National Institute of Standards and Technology, 325 Broadway, Boulder, Colorado 80305, USA*

⁶*Dipartimento di Fisica "E. Fermi," Università di Pisa, Lungarno B. Pontecorvo 3, 56122 Pisa, Italy*

(Received 11 July 2014; revised manuscript received 30 October 2014; published 24 November 2014)

Quantum engineering of time-separated Raman laser pulses in three-level systems is presented to produce an ultranarrow optical transition in bosonic alkali-earth clocks free from light shifts and with a significantly reduced sensitivity to laser parameter fluctuations. Based on a quantum artificial complex wave-function analytical model and supported by a full density-matrix simulation including a possible residual effect of spontaneous emission from the intermediate state, atomic phase shifts associated with Ramsey and hyper-Ramsey two-photon spectroscopy in optical clocks are derived. Various common-mode Raman frequency detunings are found in which the frequency shifts from off-resonant states are canceled, while their uncertainties at the 10^{-18} level of accuracy are strongly reduced.

DOI: [10.1103/PhysRevA.90.053427](https://doi.org/10.1103/PhysRevA.90.053427)

PACS number(s): 32.80.Qk, 32.80.Ee, 03.67.Lx, 42.50.Ct

I. INTRODUCTION

The control and even the cancellation of systematic frequency shifts inherent in atom-light interactions are important tasks for high-precision measurement in optical lattice clocks exploiting high-quality factors from ultranarrow transitions [1]. For instance, optical clocks avoid a dephasing of the clock states through carefully designed optical traps producing controlled ac Stark shifts of those states [2]. Engineering the phase shifts which dephase a wave function is also strongly relevant to a wide range of quantum matter experiments using trapped ions, neutral atoms, and cold molecules [3]. The standard approach for reducing those phase shifts is the decrease in the probe laser intensity. Continuous progress in the manipulation of the laser-atom or -molecule interaction has opened a new direction, quantum state engineering, in the quantum control of atomic or molecular systems [4–6]. For ultracold atoms, quantum engineering leads to the quantum simulation of Hamiltonians describing different physical systems, as in the synthesization of magnetic fields exploiting the coupling between internal and external atomic states [7–9]. Elsewhere, highly coherent and precisely controlled optical lattice clocks are explored for quantum simulation of many-body spin systems [10], and optical clock systems have been proposed to probe the many-body atomic correlation functions [11].

The present work employs the quantum engineering of atom-laser interactions to produce a perfect cancellation of the frequency shifts of a given atomic or molecular level scheme. This cancellation may be applied whenever the atomic wave-function evolution is modified by ac Stark shifts from levels both internal and external to the probed system. By making use of laser pulse sequences shaped in duration, intensity, and phase and modeled by a synthesized Hamiltonian, we easily control these shifts to a challenging 10^{-18} level of optical clock

accuracy [12]. This quantum engineering method allows us to explore various experimental conditions for optical clocks based on alkaline-earth atoms, but it can be applied to any other system dealing with a careful control of the wave-function phase shift.

Our attention is focused on the two-photon bosonic optical clocks in optical lattices with a cancellation of the clock shift at the above level of accuracy. One-photon systems such as those using fermionic species in an optical lattice clock have made great progress recently [12]. From a metrological perspective the bosonic species of optical lattice clocks have several favorable characteristics over their fermionic counterparts, e.g., simpler internal structure, distinct collision effects, and suppressed influence of higher-order lattice polarization effects. However, in order to take advantage of these benefits, a multiphoton interrogation scheme must be able to probe the atomic system without introducing significant Stark effects. The alkaline-earth fermionic species have also been useful for exploring both two- and many-body atomic interactions in a well-controlled quantum system by leveraging the clock transition as a high-precision measurement tool [10]. The same can be true of the bosonic species. However, to make such a measurement would require high-precision frequency measurements also in the bosonic systems by simultaneously activating the forbidden transition and canceling the systematic frequency shifts [13].

For two-photon optical clocks, the ac Stark shifts [14,15] are induced by a large number of off-resonant driven transitions, making their suppression very difficult to realize in a simple manner. Cancellation of the frequency shifts in those optical clocks using pulsed electromagnetically induced transparency and Raman (EIT-Raman) spectroscopic interrogation was explored in [16,17]. Alternatively, frequency shifts of one-photon clock transitions were compensated, and the uncertainty of the frequency measurement was strongly reduced using so-called hyper-Ramsey spectroscopy with two Ramsey pulses with different areas, frequencies, and phases [18]. References [19,20] pointed out that a laser frequency step applied during that pulse

*thomas.zanon@upmc.fr

sequence cancels the residual light shift and an additional echo pulse compensates both the dephasing and the uncontrolled variations of the pulse area, as in a recent $^{171}\text{Yb}^+$ ion clock experiment [21]. Within our quantum engineering approach we introduce here generalized hyper-Raman-Ramsey (HRR) techniques for two-photon optical clocks and derive the precise conditions required to operate at the 10^{-18} level of accuracy and stability. To reach this level of performance, the following criteria are sought: (i) the clock phase shift from ac Stark effects is eliminated, (ii) the shift cancellation is stable against fluctuations in the laser parameters, (iii) the Ramsey fringe contrast is maximized, and (iv) that contrast is obtained at the unperturbed clock frequency. We satisfy simultaneously all these targets with the generalized three-level HRR techniques.

We show that all the light-shift contributions to the clock transition, from internal and external states, can be canceled by operating the excitation lasers at magic detuning, more precisely a “magic” common-mode detuning for the Raman configuration. The light-shift compensation is based on control of the Bloch vector phase in the equatorial plane before the last pulse in the HRR sequence. A properly oriented vector combined with a well-chosen pulse area produces full occupation of the final state, and this condition is ideally realized within the standard Ramsey sequence [22]. However, in the presence of light shift and relaxation processes, the Bloch vector is not properly aligned, and the final pulse cannot produce the required state. Those imperfections may be compensated by a final pulse with a tuned pulse area, while the incorrect phase of the wave function is controlled by the echo pulse and, eventually, by a laser phase reversal.

Our theoretical approach is based on a non-Hermitian evolution of the atomic wave function whose phase is modified

by the ac Stark shifts from levels internal and external to the probed system. This approach enables the time-dependent solution of the atomic phase shift to be computed in analytical form, making a detailed exploration of laser parameters which cancel the frequency shifts possible. The three-level system and atomic parameters for a homogeneous medium are presented in Sec. II. We develop in Sec. III a wave-function model including radiative correction which is compared to the density-matrix results. We derive the key information on the phase shift of the wave-function particle. In Sec. IV, we synthesize a general analytical phase-shift expression between clock states leading to a frequency shift of the central fringe. In Sec. V, we develop a numerical analysis of the external light-shift contribution derived from the dynamic polarizability calculations. Finally, Sec. VI analyzes the resulting hyper-Raman Ramsey fringes produced with highly detuned two-photon pulses separated in time and the cancellation of the external light shift at particular magic detunings from the intermediate state.

II. ATOMIC PARAMETERS FOR A THREE-LEVEL SYSTEM

We examine three-level optical bosonic clocks for ^{88}Sr and ^{174}Yb with the level structure of Fig. 1(a). The doubly forbidden optical clock transition is driven by a two-photon transition between atomic states $|1\rangle \equiv |^1S_0\rangle$ and $|2\rangle \equiv |^3P_0\rangle$ via the $|3\rangle \equiv |^1P_1\rangle$ off-resonantly excited state. The $|3\rangle \rightarrow |2\rangle$ transition is driven by laser-induced magnetic coupling [23]. Our quantum engineering approach could also be applied to the magnetically induced spectroscopy scheme where a static magnetic field induces the $|3\rangle \rightarrow |2\rangle$ transition as in [24–27].

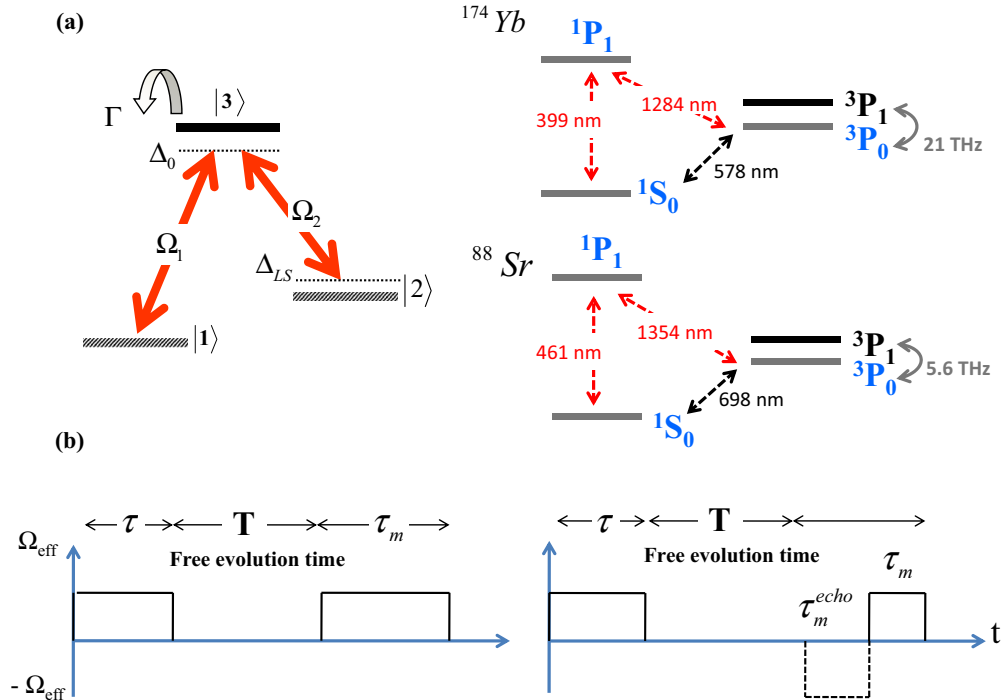


FIG. 1. (Color online) (a) Three-level atomic system configuration for spectroscopy of a forbidden atomic transition in ^{174}Yb and ^{88}Sr optical lattice clocks. Atomic parameters are described in text. (b) EIT-Raman laser pulses in a Ramsey-type (on, off, on) sequence with interrogation times τ , τ_m^{echo} (if inserting an echo pulse), and τ_m , respectively, and free evolution at the clock frequency for a time T .

TABLE I. Two-photon wave-function parameters including radiative correction.

Two-photon parameters	
Δ_{LS}	$\Delta_{\text{ext}} + (\Omega_2^2 - \Omega_1^2) \frac{\Delta_0}{\Delta_0^2 + \Gamma^2/4}$
Δ_{eff}	$\Delta_{LS} - i(\Omega_2^2 - \Omega_1^2) \frac{\Gamma/2}{\Delta_0^2 + \Gamma^2/4}$
Ω_{eff}	$2\Omega_1\Omega_2 \frac{\Delta_0 - i\Gamma/2}{\Delta_0^2 + \Gamma^2/4}$

The present work explores different laser-pulsed excitation schemes, as shown generally in Fig. 1(b), with a free-evolution time T and (eventually) an echo pulse duration τ_m^{echo} with a laser phase reversal taking place between the initial and final interrogation times, τ and τ_m , respectively. The clock transition is probed via detection of the 1S_0 or 3P_0 populations as in Ref. [16].

Within our model, the Rabi frequencies Ω_i ($i = 1, 2$) are defined by electric and magnetic dipole couplings. The laser detunings are introduced as $\Delta_1 = \Delta_0 + \eta_1$ and $\Delta_2 = \Delta_0 - \delta + \eta_2$, where Δ_0 is the common-mode frequency detuning from the excited state and δ is the Raman clock frequency detuning. η_i , the light-shift correction induced by external levels for the ($i = 1, 2$) corresponding transition, produces a correction $\Delta_{\text{ext}} = \eta_2 - \eta_1$ to the field-free clock transition. That transition also experiences an internal shift leading to the Δ_{LS} total shift listed in the first line of the Table I. The effective complex Rabi frequency Ω_{eff} of Table I determines the two-photon coupling between $|1\rangle$ and $|2\rangle$. The spontaneous emission rate from $|3\rangle$ is Γ , and optical relaxations are $\gamma_1 = \gamma_2 = \Gamma/2$. Spontaneous decays to external levels may easily be included in the model.

In order to perform an accurate analysis of the population and coherence temporal dynamics, we adopt two points of view in a bare basis: a density-matrix formalism and a complex wave-function approach. The numerical solution of the density-matrix equations of Ref. [28] allows us to examine with high accuracy the line shapes and shifts of the clock transition as in [16,18,19,21].

III. WAVE-FUNCTION ANALYSIS INCLUDING RADIATIVE CORRECTION

This section reports the formalism presented in [16,17,29] that determines the phase accumulated by the atomic wave function including all the ac Stark shifts. It is based on an effective non-Hermitian two-level Hamiltonian [30] describing the $|\Psi(t)\rangle$ superposition of the $|1\rangle, |2\rangle$ clock states,

$$|\Psi(t)\rangle = c_\alpha(t)|1\rangle + c_\beta(t)|2\rangle. \quad (1)$$

This effective wave-function model includes complex energies for open quantum systems. The model, although unadapted to conserve atomic population, is still valid as long as pulses are applied with short interaction times and any cw stationary regime is avoided. We therefore expect the spontaneous emission to have only a perturbative effect on the dynamics and choose to work in terms of the state vector $|\Psi(t)\rangle$ and its Schrödinger equation. The effects of the decoherence emission may be included by using a Δ_{eff} complex Raman detuning with

a term $-i\Gamma/2$ associated with spontaneous emission from the intermediate state inside the Δ_0 common-mode detuning. This replacement is computationally simpler than solving a full master equation. The norm of the state vector calculated using the previous assumption is not constant since after introducing a complex detuning, the Hamiltonian is no longer Hermitian. By making this replacement, we are still taking a conservative approach in the sense that this reduced-norm state vector is always less than or at least equal to the true calculation using the master equation.

The $|\Psi(t)\rangle$ evolution is driven by the Hamiltonian H ,

$$\frac{H}{\hbar} = \begin{pmatrix} 0 & \Omega_{\text{eff}} \\ \Omega_{\text{eff}} & \delta_{\text{eff}} \end{pmatrix}, \quad (2)$$

where $\delta_{\text{eff}} = -\delta + \Delta_{\text{eff}}$ and the effective complex Rabi frequency Ω_{eff} of Table I determines the two-photon coupling between $|1\rangle$ and $|2\rangle$ [31]. The Δ_{eff} detuning includes a contribution from the three-level system itself and the Δ_{ext} external light-shift contribution from others levels on the clock detuning.

Using the solution of the Schrödinger's equation, we write for the $c_{1,2}(\theta)$ transition amplitudes

$$\begin{pmatrix} c_\alpha(\theta) \\ c_\beta(\theta) \end{pmatrix} = \chi(\theta) \begin{pmatrix} M_+(\theta) & M_\dagger(\theta) \\ M_\dagger(\theta) & M_-(\theta) \end{pmatrix} \begin{pmatrix} c_\alpha(0) \\ c_\beta(0) \end{pmatrix}, \quad (3)$$

which includes a phase factor of the form

$$\chi(\theta) = \exp \left[-i \left(\frac{\Delta_0 - i\Gamma/2}{\Delta_0^2 + \frac{\Gamma^2}{4}} (\Omega_2^2 + \Omega_1^2) - \delta + \Delta_{\text{ext}} \right) \frac{t}{2} \right], \quad (4)$$

where the wave-function evolution driven by the pulse area θ is determined by the following complex 2×2 interaction matrix M [31]:

$$\begin{aligned} M(\theta) &= \begin{pmatrix} M_+(\theta) & M_\dagger(\theta) \\ M_\dagger(\theta) & M_-(\theta) \end{pmatrix} \\ &= \begin{pmatrix} \cos(\theta) + i \frac{\delta_{\text{eff}}}{\omega} \sin(\theta) & -i \frac{2\Omega_{\text{eff}}}{\omega} \sin(\theta) \\ -i \frac{2\Omega_{\text{eff}}}{\omega} \sin(\theta) & \cos(\theta) - i \frac{\delta_{\text{eff}}}{\omega} \sin(\theta) \end{pmatrix}, \quad (5) \end{aligned}$$

with $\omega^2 = \delta_{\text{eff}}^2 + \Omega_{\text{eff}}^2$. The pulsed excitation is written as a product of different matrices $M(\theta_{i,j,k})$ and a free evolution without laser light during a Ramsey time T described as a composite pulsed sequence of three different pulse areas θ_i - T - θ_j - θ_k . Pulse areas are defined by $\theta_{i,j,k} = \omega\tau_{i,j,k}/2$. with $\tau_{i,j,k} \equiv \tau, \tau_m^{\text{echo}}, \tau_m$. The final hyper-Ramsey expression is a product of matrices which depends on initials conditions $c_\alpha(0)$

and $c_\beta(0)$ as [29]

$$\begin{aligned} & \begin{pmatrix} c_\alpha(\theta_i, T, \theta_j, \theta_k) \\ c_\beta(\theta_i, T, \theta_j, \theta_k) \end{pmatrix} \\ &= \chi(\theta_i, \theta_j, \theta_k) \begin{pmatrix} M_+(\theta_i)M_+(\theta_j, \theta_k) + M_\dagger(\theta_j, \theta_k)M_\dagger(\theta_i)\exp[i\delta T] & M_\dagger(\theta_i)M_+(\theta_j, \theta_k) + M_\dagger(\theta_j, \theta_k)M_-(\theta_i)\exp[i\delta T] \\ M_\dagger(\theta_k, \theta_j)M_+(\theta_i) + M_\dagger(\theta_i)M_-(\theta_j, \theta_k)\exp[i\delta T] & M_\dagger(\theta_k, \theta_j)M_\dagger(\theta_i) + M_-(\theta_j, \theta_k)M_-(\theta_i)\exp[i\delta T] \end{pmatrix} \\ & \times \begin{pmatrix} c_\alpha(0) \\ c_\beta(0) \end{pmatrix}, \end{aligned} \quad (6)$$

where $\chi(\theta_i, \theta_j, \theta_k) = \chi(\theta_i)\chi(\theta_j)\chi(\theta_k)$ and

$$\begin{aligned} M_+(\theta_j, \theta_k) &= M_+(\theta_j)M_+(\theta_k) + M_\dagger(\theta_k)M_\dagger(\theta_j), \\ M_-(\theta_j, \theta_k) &= M_\dagger(\theta_j)M_\dagger(\theta_k) + M_-(\theta_k)M_-(\theta_j), \\ M_\dagger(\theta_j, \theta_k) &= M_\dagger(\theta_j)M_+(\theta_k) + M_\dagger(\theta_k)M_-(\theta_j), \\ M_\dagger(\theta_k, \theta_j) &= M_\dagger(\theta_k)M_+(\theta_j) + M_\dagger(\theta_j)M_-(\theta_k). \end{aligned} \quad (7)$$

IV. SYNTHESIZED PHASE SHIFT FOR LIGHT-SHIFT CONTROL

A key point for clock precision is the quantum control of the Δ_{LS} shift, with the frequency shift of the central Ramsey clock fringe approximatively given by $\delta\nu \sim \Delta_{LS}\tau/T$ for $\tau \approx \tau_m$ [22]. We show that all the light-shift contributions to the clock transition, from internal and external states, can be canceled by operating the excitation lasers at a magic common-mode detuning Δ_0^m . The optical clock applications of a synthesized shift require simultaneous cancellation and stability of the phase shift at the magic detuning, as expressed by the conditions

$$[\delta\nu]_{\Delta_0^m} = 0, \quad (8a)$$

$$\left[\frac{\partial \delta\nu}{\partial \Delta_0} \right]_{\Delta_0^m} = 0, \quad (8b)$$

$$\left[\frac{\partial^2 \delta\nu}{\partial \Delta_0^2} \right]_{\Delta_0^m} = 0. \quad (8c)$$

In analogy with quantum simulations using ultracold atoms [32], our synthesized frequency shift may be described by an effective Hamiltonian determining the final atomic state at the end of the full pulse sequence. The final expression is a hyper-Ramsey complex amplitude including initial atomic or molecular state preparation. We are then able to explicitly transition probabilities with the following general form:

$$\begin{aligned} P_{\alpha\beta} &= c_\alpha(\theta_i, T, \theta_j, \theta_k)c_\beta^*(\theta_i, T, \theta_j, \theta_k) \\ &= |\alpha_{\alpha\beta}|^2 |1 + \beta_{\alpha\beta} e^{i(\delta T + \Phi_{\alpha\beta})}|^2, \end{aligned} \quad (9)$$

using $\alpha, \beta = 1, 2$ for the state label. The complex term $\Phi_{\alpha\beta}$ represents the atomic phase shift accumulated by the wave function during the laser interrogation sequence. The wave-function expression for atomic population P_{22} of our effective

two-level system is then

$$\begin{aligned} \alpha_{22} &= [M_+(\theta_i)c_1(0) + M_\dagger(\theta_i)c_2(0)] M_\dagger(\theta_k, \theta_j)\chi(\theta_i, \theta_j, \theta_k), \\ \beta_{22} e^{i\Phi_{22}} &= \left[\frac{M_\dagger(\theta_i)c_1(0) + M_-(\theta_i)c_2(0)}{M_+(\theta_i)c_1(0) + M_\dagger(\theta_i)c_2(0)} \right] \frac{M_-(\theta_j, \theta_k)}{M_\dagger(\theta_k, \theta_j)}. \end{aligned} \quad (10)$$

The wave-function formalism adopted here with complex state energies leads to atomic phase shifts extracted from population transition probabilities. The population transition probability P_{22} is used to evaluate line shape, population transfer, and the frequency shift affecting the clock transition and is compared to a numerical density-matrix calculation describing the dynamics of a closed three-level system. For the case of a highly EIT-Raman detuned regime from the intermediate state where spontaneous emission can be neglected, including a π phase reversion of one laser field, we provide an analytical form of the associated phase shift. Starting from initial conditions $c_1(0) = 1$ and $c_2(0) = 0$, the phase shift $\Phi(^3P_0) \equiv \Phi_{22}$ is given by

$$\Phi(^3P_0) = \arg \left[\frac{M_\dagger(\theta_i) M_-(\theta_j, \theta_k)}{M_+(\theta_i) M_\dagger(\theta_k, \theta_j)} \right]. \quad (11)$$

Within the limit of $\theta_j \mapsto 0$, we recover the phase-shift expression established in Ref. [16] for an EIT-Raman excitation given by

$$\Phi(^3P_0) = \arg \left[\frac{M_\dagger(\theta_i) M_-(\theta_k)}{M_+(\theta_i) M_\dagger(\theta_k)} \right]. \quad (12)$$

The phase shift $\Phi(^3P_0)$ determines the optical lattice clock shift $\delta\nu(\Delta_0)$ measured on the central fringe in the two-photon HRR spectroscopy. When $T \gg \tau, \tau_m^{\text{echo}}, \tau_m$, that shift is given by

$$\delta\nu(\Delta_0) \approx -\frac{\Phi(^3P_0)}{2\pi T}. \quad (13)$$

In the $\Delta_0 \gg \Gamma$ regime, the role of spontaneous emission is strongly reduced, and the population transfer to the excited state is negligible. In this case, the clock phase shift depends only on pulse area. The full expression of the $\Phi(^3P_0)$ phase shift corresponding to a composite sequence of three different laser pulse areas $\theta_i, \theta_j, \theta_k$ including a π phase reversion during

the second pulse is

$$\Phi(^3P_0) = -\arctan \left[\frac{\frac{\Delta_{\text{eff}}}{\omega} \left(\frac{\tan \theta_j + \tan \theta_k}{1 + \frac{\Omega_{\text{eff}}^2 - \Delta_{\text{eff}}^2}{\omega^2} \tan \theta_j \tan \theta_k} + \frac{\tan \theta_j - 2 \frac{\tan \theta_j \tan \theta_k}{\tan \theta_j - \tan \theta_k}}{1 + 2 \frac{\Delta_{\text{eff}}^2}{\omega^2} \frac{\tan \theta_j \tan \theta_j \tan \theta_k}{\tan \theta_j - \tan \theta_k}} \right)}{1 - \left(\frac{\Delta_{\text{eff}}}{\omega} \right)^2 \frac{\tan \theta_j + \tan \theta_k}{1 + \frac{\Omega_{\text{eff}}^2 - \Delta_{\text{eff}}^2}{\omega^2} \tan \theta_j \tan \theta_k} \frac{\tan \theta_j - 2 \frac{\tan \theta_j \tan \theta_k}{\tan \theta_j - \tan \theta_k}}{1 + 2 \frac{\Delta_{\text{eff}}^2}{\omega^2} \frac{\tan \theta_j \tan \theta_j \tan \theta_k}{\tan \theta_j - \tan \theta_k}}} \right]. \quad (14)$$

When the second pulse area is $\theta_j \mapsto 0$ and $\theta_i \neq \theta_k$, we recover the full expression of the hyper-Ramsey phase-shift expression derived perturbatively in [18] for a two-level system:

$$\Phi(^3P_0) = -\arctan \left[\frac{\frac{\Delta_{\text{eff}}}{\omega} (\tan \theta_i + \tan \theta_k)}{1 - \left(\frac{\Delta_{\text{eff}}}{\omega} \right)^2 \tan \theta_i \tan \theta_k} \right] \quad (15a)$$

$$= -\arctan \left[\frac{\Delta_{\text{eff}}}{\omega} \tan \theta_i \right] - \arctan \left[\frac{\Delta_{\text{eff}}}{\omega} \tan \theta_k \right]. \quad (15b)$$

Based on Ref. [33], Eqs. 15(a) and 15(b) are fully equivalent. Note that Eq. (14) also exhibits this remarkable mathematical form. For the well-known Ramsey configuration [22] where $\theta_i = \theta_k = \theta$, that shift is

$$\Phi(^3P_0) = -\arctan \left[\frac{2 \frac{\Delta_{\text{eff}}}{\omega} \tan \theta}{1 - \left(\frac{\Delta_{\text{eff}}}{\omega} \right)^2 \tan^2 \theta} \right] \quad (16a)$$

$$= -2 \arctan \left[\frac{\Delta_{\text{eff}}}{\omega} \tan \theta \right]. \quad (16b)$$

From a geometrical point of view, this Ramsey phase shift is exactly two times the Eulerian angle accumulated by a Bloch vector projection of rotating components in the complex plane using a two-dimensional Cauley-Klein representation of the spin-1/2 rotational group [34,35].

V. LIGHT-SHIFT NUMERICAL ANALYSIS

The light shift Δ_{LS} of the clock states containing contributions from the three-level system itself and the Δ_{ext} contribution is written as

$$\begin{aligned} \Delta_{\text{LS}} &= (\Delta_2^{\text{res}} - \Delta_1^{\text{res}}) + \Delta_{\text{ext}} \\ &= (\Delta_2^{\text{res}} - \Delta_1^{\text{res}}) + (\eta_2 - \eta_1), \end{aligned} \quad (17)$$

where η_i defines the external contribution from the i th level. The near-resonant light shift may be written as

$$\begin{aligned} \Delta_i^{\text{res}} &= \frac{\Delta_0}{\Delta_0^2 + \Gamma^2/4} \Omega_i^2 \\ &= \frac{\Delta_0}{\Delta_0^2 + \Gamma^2/4} \left(\frac{|\langle i|\mathbf{d}|3\rangle|}{\hbar} \right)^2 \left(\frac{E_{L,i}}{2} \right)^2, \end{aligned} \quad (18)$$

with $i = 1, 2$. Here we have introduced the $E_{L,i}$ electric ($B_{L,i}$ magnetic) field amplitude for the i th laser field and the $\langle i|\mathbf{d}|3\rangle$ ($\langle i|\mathbf{m}|3\rangle$) electric (magnetic) dipole operator between the $|i\rangle$ state and the $|3\rangle = |n^1P_0\rangle$ intermediate state with $n = 5, 6$ for Sr and Yb, respectively.

The evaluation of the external contribution requires the dipole moment matrix elements and the energy position for

all the excited states. However, it should be noticed that the above Δ_{LS} quantity is also calculated to determine the magic wavelength in the design of optical traps producing controlled Sr or Yb frequency shifts. We use the definition of Refs. [1,36] for the $\alpha_i(\omega)$ dynamic polarizabilities of the $i = 1, 2$ states associated with a laser field at angular frequency ω ,

$$\alpha_i(\omega) = \sum_n \frac{|\langle i|\mathbf{d}|n\rangle|^2}{3} \left[\frac{1}{E_n - E_i - \hbar\omega} + \frac{1}{E_n - E_i + \hbar\omega} \right], \quad (19)$$

with \mathbf{d} again being the electric dipole operator (or the \mathbf{m} magnetic dipole moment for the electric dipole forbidden transitions) and with the summation over a complete set of atomic states. We neglect, in this analysis, higher-order dynamic polarizabilities. Using the above polarizabilities, the light shift of the $|1\rangle$ - $|2\rangle$ transition is

$$\Delta_{\text{LS}}(\omega) = \alpha_1(\omega) \left(\frac{E_{L,1}}{2} \right)^2 - \alpha_2(\omega) \left(\frac{E_{L,2}}{2} \right)^2. \quad (20)$$

For each $i = 1, 2$ state the sum of Eq. (19) includes only one near-resonant light shift, while all the remaining ones represent the external light shift. Within that sum and following Eqs. (17) and (18), we separate the resonant contribution from the remaining ones denoted by $\tilde{\alpha}_i$

$$\alpha_i(\omega) = \tilde{\alpha}_i(\omega) + \frac{\Delta_0}{\Delta_0^2 + \Gamma^2/4} \left(\frac{|\langle i|\mathbf{d}|3\rangle|}{\hbar} \right)^2, \quad (21)$$

where

$$\begin{aligned} \tilde{\alpha}_i(\omega) &= \sum_{n \neq 3} \frac{|\langle i|\mathbf{d}|n\rangle|^2}{3} \left[\frac{1}{E_n - E_i - \hbar\omega} + \frac{1}{E_n - E_i + \hbar\omega} \right] \\ &\quad + \frac{|\langle i|\mathbf{d}|3\rangle|^2}{3} \frac{1}{E_3 - E_i + \hbar\omega}. \end{aligned} \quad (22)$$

The combination of Eqs. (17), (20), and (22) allows us to derive the Δ_i^{ext} light-shift contribution. We have calculated from the analysis reported in Refs. [37,38] the $\tilde{\alpha}_i$ external levels' dynamic polarizabilities at the laser frequencies required for the EIT-Raman and hyper-Ramsey schemes investigated in the present work, as reported in Table II. The η_i light-shift contributions of the external levels in the last column of Table II are obtained from $\tilde{\alpha}_i$ using the conversion factor of Ref. [1]. The η_i light shifts are computed in millihertz for a laser intensity of 1 mW/cm².

TABLE II. Sr and Yb atomic levels for the two-photon clock investigated in the present work. The coupling to the $|3\rangle = |nsnp\ ^1P_1\rangle$ state is either an electric dipole or a magnetic dipole transition. For the $i = 1, 2$ level the α_i external light-shift contribution is in atomic units in the next to last column, with η_i in the last column.

Atom	$ 1\rangle$ or $ 2\rangle$	$ 3\rangle$	λ (nm)	$\omega/2\pi$	$\langle 1 \mathbf{d} 3\rangle$ or $\langle 2 \mathbf{m} 3\rangle$ (a.u.)	$\tilde{\alpha}_i$ (a.u.)	η_i [mHz/(mW/cm ²)]
Sr	$ 1\rangle = 5^1S_0\rangle$	$ 5^1P_0\rangle$	461	650.5	$\langle 1 \mathbf{d} 3\rangle = 5.248(2)$ [39]	48.5	-2.27
Sr	$ 1\rangle = 5^1S_0\rangle$	$ 5^1P_0\rangle$	1354	221.2	$\langle 1 \mathbf{d} 3\rangle = 5.248(2)$ [39]	213.6	-10.01
Sr	$ 2\rangle = 5^3P_0\rangle$	$ 5^1P_0\rangle$	461	650.6	$\langle 2 \mathbf{m} 3\rangle = 0.022\mu_B$ [23]	-1220.9	57.22
Sr	$ 2\rangle = 5^3P_0\rangle$	$ 5^1P_0\rangle$	1354	221.2	$\langle 2 \mathbf{m} 3\rangle = 0.022\mu_B$ [23]	61.8	-2.90
Yb	$ 1\rangle = 6^1S_0\rangle$	$ 6^1P_0\rangle$	399	751.5	$\langle 1 \mathbf{d} 3\rangle = 4.148(2)$ [40]	33.0	-1.55
Yb	$ 1\rangle = 6^1S_0\rangle$	$ 6^1P_0\rangle$	1284	233.2	$\langle 1 \mathbf{d} 3\rangle = 4.148(2)$ [40]	152.9	-7.14
Yb	$ 2\rangle = 6^3P_0\rangle$	$ 6^1P_0\rangle$	399	751.5	$\langle 2 \mathbf{m} 3\rangle = 0.16$ [41]	-129.1	6.05
Yb	$ 2\rangle = 6^3P_0\rangle$	$ 6^1P_0\rangle$	1284	233.2	$\langle 2 \mathbf{m} 3\rangle = 0.16$ [41]	-944.4	44.26

VI. APPLICATION TO BOSONIC OPTICAL LATTICE CLOCKS

We have applied the density-matrix and complex wavefunction approaches to the light-shift control for several HRR clock interrogation parameters; the Δ_{ext} external shift contributions and the magic detunings are reported in Table III. Different examples of shift cancellation with a fringe contrast nearly equal to 1 in the absence of spontaneous emission are presented in the left panels of Fig. 2. Results for the synthesized $\delta\nu(\Delta_0)$ dependence on change in selected laser parameters are presented in the right panels of Fig. 2 and in Fig. 3, which includes spontaneous emission for different laser-pulsed excitation schemes. The Ramsey sequence of Fig. 2(a) with $\tau_m = \tau \ll T$ and $\tau_m^{\text{echo}} \mapsto 0$ produces the quasilinear $\delta\nu$ dependence on $\Delta_0 = 0$ in the right panel: only the $\delta\nu(\Delta_0^m) = 0$ condition of Eqs. (8) is satisfied. The HRR sequence of Fig. 2(b) produces a $\delta\nu(\Delta_0)$ cubic dependence, providing an excellent compensation and stability of the phase shift. The HRR + phase scheme generalizing the two-level scheme of [18], where the laser pulse sequence includes a phase reversal during the second pulse scheme, produces a synthesized plateau against fluctuations in the laser frequency around the magic detuning, as in the right panel of Fig. 2(c). Note that the associated fringes still

TABLE III. Various sets of Raman interaction parameters including laser intensities I_1, I_2 and pulse durations (τ, τ_m) , at fixed $T = 5$ s, for ^{88}Sr and ^{174}Yb two-photon interrogation leading to the listed Δ_0^m magic detuning.

	^{88}Sr				
	set 1	set 2	set 3	set 4	set 5
I_1 (mW/cm ²)	0.066	0.016	4.2	160	640
I_2 (W/cm ²)	9.4	2.35	37.4	57.2	229
$\Delta_{\text{ext}}/2\pi$ (Hz)	66	17	267	417	1667
(τ, τ_m) (s)	$(\frac{3}{16}, \frac{9}{16})$	$(\frac{3}{4}, \frac{9}{4})$	$(\frac{3}{16}, \frac{9}{16})$	$(\frac{3}{5}, \frac{9}{5})$	$(\frac{3}{20}, \frac{9}{20})$
$\Delta_0^m/2\pi$ (GHz)	11.2	11.2	179	4370	4370
	^{174}Yb				
	set 1	set 2	set 3	set 4	set 5
I_1 (mW/cm ²)	0.78	0.2	12.5	122	487
I_2 (W/cm ²)	1.3	0.32	5.2	8.1	32.3
$\Delta_{\text{ext}}/2\pi$ (Hz)	66	17	267	417	1667
(τ, τ_m) (s)	$(\frac{3}{32}, \frac{9}{32})$	$(\frac{3}{8}, \frac{9}{8})$	$(\frac{3}{64}, \frac{9}{64})$	$(\frac{3}{40}, \frac{9}{40})$	$(\frac{3}{160}, \frac{9}{160})$
$\Delta_0^m/2\pi$ (GHz)	82	82	326.7	2037	2037

have the maximum contrast. Magic detunings for other HRR interrogation parameters can be found in Table III.

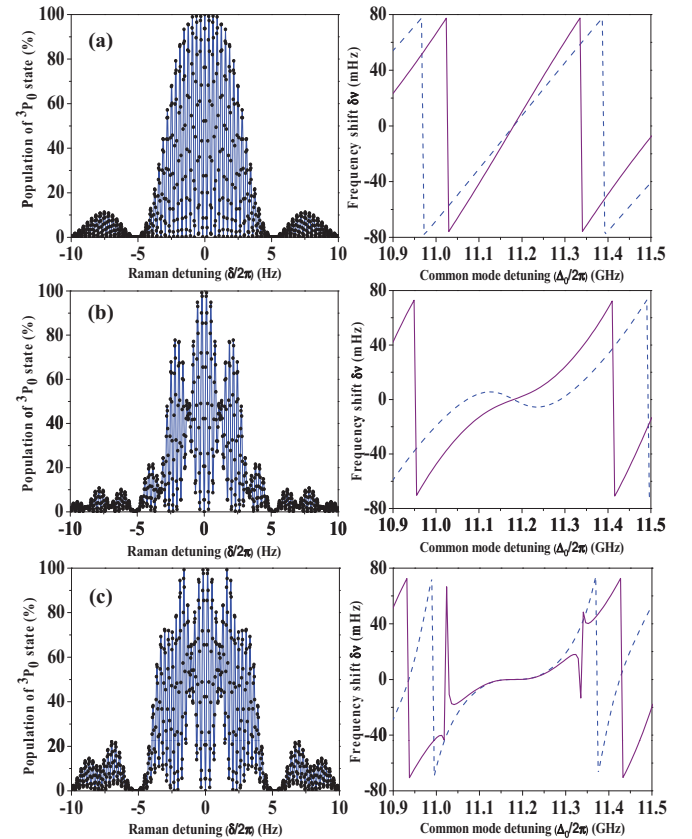


FIG. 2. (Color online) (left) ^{88}Sr transition probabilities measured on the 3P_0 clock state and (right) $\delta\nu$ frequency shifts vs the common-mode detuning Δ_0 for different operating parameters all satisfying the primary condition $\delta\nu(\Delta_0^m) = 0$. Rabi frequencies $\Omega_1 = 20\sqrt{\pi}\Delta_0^m/3$ and $\Omega_2 = \Omega_1/100$, free evolution time $T = 3$ s, and pulse duration $\tau = 0.1875 = 3/16$ s. In the right panels, the frequency shifts are shown with a relative $\pm 10\%$ pulse area variation (solid and dashed lines). All $\delta\nu(\Delta_0)$ curves are computed from Eq. (14). (a) Ramsey spectroscopy based on the $\pi/2$ - T - $\pi/2$ laser pulse sequence. (b) HRR scheme with the $\pi/2$ - T - $3\pi/2$ pulse sequence. (c) HRR + phase and echo scheme with the $\pi/2$ - T - π - $\pi/2$ pulse sequence including a phase reversal during the second pulse. In this case, a plateau is obtained around a magic common-mode Raman detuning $\Delta_0^m/2\pi \sim 11.2$ GHz, with all conditions of Eqs. (8) satisfied.

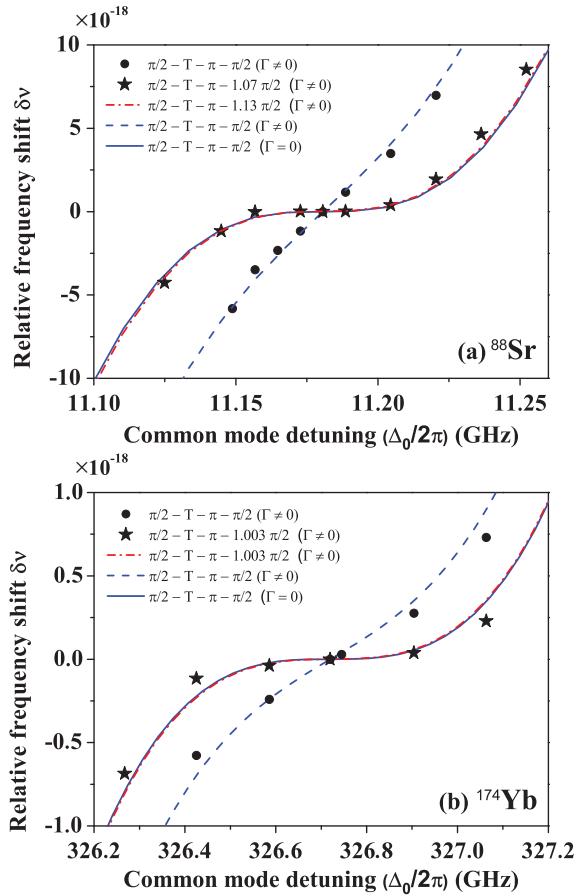


FIG. 3. (Color online) Fractional frequency shift (in 10^{-18} unit) based on a $\pi/2$ - T - $3\pi/2$ laser pulse sequence in the presence of spontaneous emission relaxation. All conditions from Eqs. (8) are fulfilled at the millihertz level by adding, between the preparation and detection pulses, an echo pulse with a duration $\tau_m^{\text{echo}} = 2\tau$, reversing the sign of one Rabi frequency. (a) ^{88}Sr clock frequency shift around $\Delta_0^m = 11.2$ GHz with $\Gamma/2\pi = 32$ MHz and (b) ^{174}Yb clock frequency shift around $\Delta_0^m = 326.7$ GHz with $\Gamma/2\pi = 28.9$ MHz. The density matrix analyzes (solid dots and stars) are reproduced by the complex wave-function model (dashed and solid lines). Rabi frequencies are as in Fig. 2; free evolution time $T = 5$ s.

Our synthesized light-shift approach allows the realization of shift cancellation with insensitivity to fluctuations of the laser intensity and/or pulse duration. For instance, the HRR + phase scheme suffers from an unstable shift compensation as a function of pulse area. That shift dependence on the pulse area is strongly eliminated within the synthesized phase shift approach using an additional echo pulse with phase reversal.

The $\Omega_{\text{eff}} \rightarrow -\Omega_{\text{eff}}$ phase shift is introduced within the first part of the second pulse, which is divided in two parts with areas π and $\pi/2$, respectively. A very high stability against laser intensity was verified.

Figures 2 and 3 examine clock interrogation with Δ_0^m frequency detunings in the gigahertz range, i.e., in a regime where the approximation of $\Gamma \mapsto 0$ should be good enough. However, a density-matrix numerical simulation (fully confirmed by the wave-function model) pointed out that the spontaneous emission rate from the excited state cannot be

totally neglected, as in [20] for a two-level system. The HRR results shown by the dots and dashed line in Fig. 3 for ^{88}Sr and ^{174}Yb point out that at the magic detuning the slope $\partial\delta\nu/\partial\Delta_0$ is now different from zero, significantly compromising the insensitivity of the cancellation to laser fluctuations. The relaxation introduces into the ω effective frequency a phase shift modifying the coherent evolution of the atomic wave function. The insensitivity is recovered by applying an HRR+Phase with an echo sequence and a finely tuned length of the third detection pulse, $\pi + 1.07\pi/2$ for ^{88}Sr at magic detuning $\Delta_0^m = 11.2$ GHz and $\pi + 1.003\pi/2$ for ^{174}Yb at $\Delta_0^m = 326.7$ GHz, as shown by stars (density matrix) and solid lines (wave-function model) in Fig. 3.

VII. CONCLUSION

Our wave-function approach is very efficient for deriving the clock shift under different operating conditions and determining the laser parameters for the optical clock shift cancellation at the millihertz level. We present its application to a hyper-Raman-Ramsey spectroscopic method based on two pulses with areas $\pi/2$ and $3\pi/2$ that cancels the light shift and efficiently suppresses the sensitivity to laser field fluctuations without the additional frequency step in the laser frequency required in Refs. [19–21].

HRR spectroscopy has broader applications than light-shift cancellation control in clocks, which focus on the idea of quantum engineering of internal atomic and molecular states to prepare and probe complex quantum systems. Synthesized phase shifts and operation at a magic Raman detuning could be applied to all high-precision measurement using Ramsey spectroscopy, such as in testing the potential variation of fundamental constants with time [42], in high-precision mass spectrometry with Penning traps [43,44], or in measuring gravitationally induced quantum phase shifts for neutrons [45]. The light-insensitive two-photon approach could also be applied to molecular optical clocks sensitive to potential variation in the electron-to-proton mass ratio [46]. In atomic interferometry, stimulated Raman transitions are intensively used to realize accurate inertial sensors but still suffer from imprecise light-shift control [47]. Our technique would be able to strongly suppress these systematic effects and could be more selective in the velocity class of atoms with less dispersion when atomic recoil and Doppler effects are included. In time and frequency standards, there continues to be a significant effort to push miniaturized microwave clock performance to higher levels, with most methods employing a three-level coherent-population-trapping (CPT) interrogation. The HRR scheme may have a significant impact on all pulsed CPT-Raman clock designs [48,49] and also in the case of the recently proposed *E1-M1* portable optical clock [50].

ACKNOWLEDGMENTS

We gratefully acknowledge J. Lodewyck for providing Sr scalar polarizabilities to check the desired clock accuracy, K. Bely for an estimate of magnetic dipole coupling in Yb, and M. Glass-Maujean and C. Janssen for a careful reading of the manuscript.

- [1] A. Derevianko and H. Katori, *Rev. Mod. Phys.* **83**, 331 (2011).
- [2] J. Ye, H. J. Kimble, and H. Katori, *Science* **320**, 1734 (2008).
- [3] M. Kajita, G. Gopakumar, M. Abe, and M. Hada, *Phys. Rev. A* **84**, 022507 (2011).
- [4] K. Gibble, *Phys. Rev. Lett.* **103**, 113202 (2009).
- [5] W. Mainault, C. Deutsch, K. Gibble, J. Reichel, and P. Rosenbusch, *Phys. Rev. Lett.* **109**, 020407 (2012).
- [6] E. L. Hazlett, Y. Zhang, R. W. Stites, K. Gibble, and K. M. O'Hara, *Phys. Rev. Lett.* **110**, 160801 (2013).
- [7] Y.-J. Lin, R. L. Compton, K. Jiménez-García, J. V. Porto, and I. B. Spielman, *Nature (London)* **462**, 628 (2009).
- [8] M. Aidelsburger, M. Atala, M. Lohse, J. T. Barreiro, B. Paredes, and I. Bloch, *Phys. Rev. Lett.* **111**, 185301 (2013).
- [9] H. Miyake, G. A. Siviloglou, C. J. Kennedy, W. C. Burton, and W. Ketterle, *Phys. Rev. Lett.* **111**, 185302 (2013).
- [10] M. J. Martin, M. Bishof, M. D. Swallows, X. Zhang, C. Benko, J. von-Stecher, A. V. Gorshkov, A. M. Rey, and Jun Ye, *Science* **341**, 632 (2013); X. Zhang, M. Bishof, S. L. Bromley, C. V. Kraus, M. S. Safronova, P. Zoller, A. M. Rey, and J. Ye, *ibid.* **345**, 1467 (2014).
- [11] M. Knap, A. Kantian, T. Giamarchi, I. Bloch, M. D. Lukin, and E. Demler, *Phys. Rev. Lett.* **111**, 147205 (2013).
- [12] R. Le Targat *et al.*, *Nat. Commun.* **4**, 2109 (2013); N. Hinkley, J. A. Sherman, N. B. Phillips, M. Schioppo, N. D. Lemke, K. Bely, M. Pizzocaro, C. W. Oates, and A. D. Ludlow, *Science* **341**, 1215 (2013); B. J. Bloom, T. L. Nicholson, J. R. Williams, S. L. Campbell, M. Bishof, X. Zhang, W. Zhang, S. L. Bromley, and J. Ye, *Nature (London)* **506**, 71 (2014).
- [13] A. D. Ludlow, M. M. Boyd, J. Ye, E. Peik, and P. O. Schmidt, *arXiv:1407.3493*.
- [14] P. F. Liao and J. E. Bjorkholm, *Phys. Rev. Lett.* **34**, 1 (1975).
- [15] C. Cohen-Tannoudji, *Metrologia* **13**, 161 (1977).
- [16] T. Zanon-Willette, A. D. Ludlow, S. Blatt, M. M. Boyd, E. Arimondo, and J. Ye, *Phys. Rev. Lett.* **97**, 233001 (2006).
- [17] T. H. Yoon, *Phys. Rev. A* **76**, 013422 (2007).
- [18] V. I. Yudin, A. V. Taichenachev, C. W. Oates, Z. W. Barber, N. D. Lemke, A. D. Ludlow, U. Sterr, Ch. Lisdat, and F. Riehle, *Phys. Rev. A* **82**, 011804(R) (2010).
- [19] A. V. Taichenachev *et al.*, *JETP Lett.* **90**, 713 (2009).
- [20] K. S. Tabatchikova, A. V. Taichenachev, and V. I. Yudin, *JETP Lett.* **97**, 311 (2013).
- [21] N. Huntemann, B. Lipphardt, M. Okhapkin, Chr. Tamm, E. Peik, A. V. Taichenachev, and V. I. Yudin, *Phys. Rev. Lett.* **109**, 213002 (2012).
- [22] N. F. Ramsey, *Phys. Rev.* **78**, 695 (1950); *Molecular Beams* (Clarendon, Oxford, 1956).
- [23] R. Santra, E. Arimondo, T. Ido, C. H. Greene, and J. Ye, *Phys. Rev. Lett.* **94**, 173002 (2005).
- [24] A. V. Taichenachev, V. I. Yudin, C. W. Oates, C. W. Hoyt, Z. W. Barber, and L. Hollberg, *Phys. Rev. Lett.* **96**, 083001 (2006).
- [25] Z. W. Barber, C. W. Hoyt, C. W. Oates, L. Hollberg, A. V. Taichenachev, and V. I. Yudin, *Phys. Rev. Lett.* **96**, 083002 (2006).
- [26] X. Baillard *et al.*, *Opt. Lett.* **32**, 1812 (2007).
- [27] T. Akatsuka, M. Takamoto, and H. Katori, *Phys. Rev. A* **81**, 023402 (2010).
- [28] T. Zanon-Willette, E. de Clercq, and E. Arimondo, *Phys. Rev. A* **84**, 062502 (2011).
- [29] T. Zanon-Willette, Ph.D. thesis, Laboratoire national de métrologie et d'essais–Système de Références Temps-Espace and Université Pierre et Marie Curie, 2005.
- [30] H. Carmichael, *An Open System Approach to Quantum Optics* (Springer, Berlin, 1993).
- [31] Two-photon detunings and the effective Rabi frequency of our matrix elements have the opposite sign of those in [16].
- [32] I. Bloch, J. Dalibard, and S. Nascimbène, *Nat. Phys.* **8**, 267 (2012).
- [33] M. Abramowitz and I. A. Stegun, *Handbook of Mathematical Functions* (Dover, New York, 1968).
- [34] E. T. Jaynes, *Phys. Rev.* **98**, 1099 (1955).
- [35] R. L. Schoemaker, in *Laser Coherence Spectroscopy*, edited by J. I. Steinfeld (Plenum, New York, 1978), p. 197.
- [36] V. A. Dzuba and A. Derevianko, *J. Phys. B* **43**, 074011 (2010).
- [37] M. S. Safronova, S. G. Porsev, and C. W. Clark, *Phys. Rev. Lett.* **109**, 230802 (2012).
- [38] M. S. Safronova, S. G. Porsev, U. I. Safronova, M. G. Kozlov, and C. W. Clark, *Phys. Rev. A* **87**, 012509 (2013).
- [39] M. Yasuda, T. Kishimoto, M. Takamoto, and H. Katori, *Phys. Rev. A* **73**, 011403(R) (2006).
- [40] Y. Takasu, K. Komori, K. Honda, M. Kumakura, T. Yabuzaki, and Y. Takahashi, *Phys. Rev. Lett.* **93**, 123202 (2004).
- [41] K. Bely (private communication).
- [42] E. R. Hudson, H. J. Lewandowski, B. C. Sawyer, and J. Ye, *Phys. Rev. Lett.* **96**, 143004 (2006).
- [43] G. Bollen, H.-J. Kluge, T. Otto, G. Savard, and H. Stolzenberg, *Nucl. Instrum. Methods Phys. Res., Sect. B* **70**, 490 (1992).
- [44] M. Kretzschmar, *Int. J. Mass Spectrom.* **264**, 122 (2007).
- [45] H. Abele, T. Jenke, H. Leeb, and J. Schmiedmayer, *Phys. Rev. D* **81**, 065019 (2010).
- [46] J.-Ph. Karr, *J. Mol. Spectrosc.* **300**, 37 (2014).
- [47] A. Gauguier, T. E. Mehlstäubler, T. Lévêque, J. Le Gouët, W. Chaïbi, B. Canuel, A. Clairon, F. Pereira, Dos Santos, and A. Landragin, *Phys. Rev. A* **78**, 043615 (2008).
- [48] J. Vanier, *Appl. Phys. B* **81**, 421 (2005).
- [49] V. Shah and J. Kitching, *Adv. At. Mol. Opt. Phys.* **59**, 21 (2010).
- [50] E. A. Alden, K. R. Moore, and A. E. Leanhardt, *Phys. Rev. A* **90**, 012523 (2014).